FLOW ANALOGY OF PSEUDOPLASTIC LIQUID IN GEOMETRICALLY SIMILAR STIRRED VESSELS BASED ON NUMERICAL ANALYSIS

MEGURU KAMINOYAMA
JGC Corporation, Yokohama 232
Department of Material Science and Chemical Engineering, Yokohama National University, Yokohama 240
FUMIO SAITO AND MITSUO KAMIWANO
Department of Material Science and Chemical Engineering, Yokohama National University, Yokohama 240

Key Words: Agitation, Numerical Analysis, Pseudoplastic Liquids, Ellis Model, Stirred Vessels, Flow Analogy, Scale-Up

Three-dimensional numerical analysis of flow behaviour such as velocity components, shear rate and apparent viscosity of a highly viscous pseudoplastic Ellis liquid in stirred vessels was performed. The vessels used were geometrically similar, non-baffled ones of 0.2 to 0.8 m vessel diameter each with a 6-blade turbine, a paddle and an anchor-type stirring impeller.

The analogy of flow fields in model and large-scale stirred vessels was investigated by applying the concept of representative shear rate to estimate the apparent viscosity of a power-law fluid proposed by Metzner *et al.* and Nagata. It was found that the normalized flow profiles of a pseudoplastic liquid in the scaled-up vessels were nearly consistent with those in the model vessel within the impeller blade region, while it was quantitatively shown that the deviation between the two profiles in the outer region of the impeller expands with increasing vessel diameter.

Introduction

The estimation of flow behaviour of liquid in a stirred vessel is essential not only for the optimun mixing operation but also for the suitable design of a mixing device. It is also important to know how the flow analogy of a pseudoplastic liquid can be applied to the scale-up of a stirred vessel, since the viscosity of the liquid is dependent on the shear rate so that the flow of liquid in a mixer is more complicated than that of a Newtonian liquid. But it is not always easy to measure the flow velocity components precisely in the whole region of a stirred vessel. Thus, there are hardly any detailed data on the three-dimensional flow velocity components in a large-scale mixer. The flow analogy of the liquid has been much less adequately understood. On the other hand, numerical analysis could provide a complete understanding of the flow field in a stirred vessel within the fluid region where an assumed rheological model is applicable. From this point of view, some numerical analyses have been attempted in a two-dimensional flow field of non-Newtonian liquids regarding the analogy law of flow fields by Hiraoka *et al.*[2] and that of power consumption by Bertrand *et al.*[1] The authors proposed a method for numerically analysing the three-dimensional flow behaviour of the pseudoplastic Ellis liquid in a stirred vessel with a turbine impeller in a previous paper.[3] In that work the proposed method was applied to a mixer of 0.2 m vessel diameter, and the reliability of the method was proved by the close agreement of the simulation results with experimental data by means of a dual-type image-sensor velocimeter.[4-6] Following the previous paper, firstly a similar calculation of the flow velocity has been carried out in the model vessel of 0.2 m diameter with two other types of impeller such as a 6-blade paddle and an anchor. Secondly, the scale-up criterion with respect to the flow analogy has been examined by applying the concept of representative shear rate for estimating apparent viscosity proposed by Metzner *et al.*[7,8] and Nagata[9] to geometrically similar scaled-up vessels up to 0.8 m vessel diameter.

* Received April 15, 1989. Correspondence concerning this article should be addressed to M. Kaminoyama.

1. Analysis

In the case of a Newtonian fluid, Eq. (1) is usually applied as a criterion for the scale-up of a stirred vessel.

$$n_m d_m^{\beta} = n_l d_l^{\beta} \tag{1}$$

where n is the rotational speed of impeller, and d the impeller diameter, subscripts m and l respectively indicate model and large-scale vessel and β is the index. When β is set equal to 0, 2/3, or 1, Eq. (1) corresponds to the scale-up criterion when the rotational speed of the impeller, the power consumption per unit volume,

and the impeller tip velocity respectively is held constant. When β is 2, Eq. (1) is equivalent to the scale-up criterion on the basis of the impeller Reynolds number for the Newtonian liquid, Re_d, given by Eq. (2), due to the constancy of density, ρ, and viscosity, μ, of the liquid in the whole region of the vessel.

$$Re_d=\frac{\rho n d^2}{\mu} \tag{2}$$

The analogy of the flow fields for a Newtonian fluid is therefore attained when $\beta=2$ in Eq. (1), which was also confirmed by the authors' numerical calculations.*

For a non-Newtonian fluid like a pseudoplastic liquid, however, it is impossible to obtain a similar velocity profile[10] in differently sized vessels by this approach, because the non-Newtonian viscosity, η, depending on the shear rate, which is determined from the flow velocity distribution, varies complicatedly in a mixer. The problem is how to define the representative shear rate in the mixer, Γ, in order to calculate η which is substituted for μ in Eq. (2). Metzner *et al.*[7,8] proposed the power correlation method for a power-law fluid from which the apparent viscosity can be calculated by the average shear rate in a mixer, Γ, which is proportional to the rotational speed of the impeller as given by Eq. (3).

$$\Gamma=Bn \tag{3}$$

Where B is a constant value depending on the type of impeller and is determined experimentally through the power correlation with a Newtonian liquid. The power consumption is fundamentally based on the flow velocity distribution in a stirred vessel. Eq. (3) is therefore considered to be also applicable to the analogy of flow fields. Re_d for a non-Newtonian liquid is accordingly rewritten as Eq. (4).

$$Re_d=\frac{\rho n d^2}{\eta\big|_{\Gamma=Bn}} \tag{4}$$

The Ellis model given by Eq. (5) is used in this paper to express the pseudoplasticity of the liquid.

$$\left(\frac{\sqrt{\frac{1}{2}(\Delta:\Delta)}}{\tau_{1/2}}\right)^{\alpha-1}\cdot\eta^{\alpha}+\eta-\eta_0=0 \tag{5}$$

The rotational speed of impeller in the large-scale vessel, n_l, can therefore be determined by fitting Re_d for the model and the large-scale vessels as follows.

$$n_l=n_m\left(\frac{\eta_l}{\eta_m}\right)\left(\frac{d_m}{d_l}\right)^2 \tag{6}$$

η_m in Eq. (6) is calculated from Eq. (7), which is obtained by substituting Bn_m for $\sqrt{\frac{1}{2}(\Delta:\Delta)}$ in Eq. (5).

$$\left(\frac{Bn_m}{\tau_{1/2}}\right)^{\alpha-1}\cdot\eta_m^{\alpha}+\eta_m-\eta_0=0 \tag{7}$$

Similarly, η_l is calculated from Eq. (8) with η_m.

$$\left(\frac{Bn_m d_m^2}{\tau_{1/2}\eta_m d_l^2}\right)^{\alpha-1}\cdot\eta_l^{2\alpha-1}+\eta_l-\eta_0=0 \tag{8}$$

In this paper, the authors investigate the applicability of the Reynolds number determined by Eq. (4) to the analogy law regarding the flow velocity distribution. The values of B for the power correlation proposed by Metzner *et al.*[7,8] and Nagata[9] are used in the calculation of Eqs. (7) and (8) for the discussion of flow analogy.

2. Calculation Conditions

The numerical method was reported in the previous paper.[3] **Figure 1** shows the scheme of mixers, each with three types of impeller (turbine (a), paddle (b) and anchor (c)), and their analysed regions. Successive regions are 1/12, 1/6, and one-half of the vessel in turn, due to considerations of the symmetry of each vessel. They are divided into $20\times6\times20$, $20\times6\times40$, and $20\times9\times20$ cells** in r, θ, and z directions respectively. In the range of n in this paper, the liquid surfaces in the mixers without baffle are kept approximately flat. Consequently, the flow analysis of the liquid is advanced without any consideration of the influence of Froude number on the flow analogy. The pseudoplastic liquid taken for the analysis is a 1.2 wt% aqueous solution of hydroxyethyl cellulose. The three constant parameters composing the Ellis model equation, α, $\tau_{1/2}$, and η_0, are determined experimentally as 2.85, 23.3 Pa, and 1.88 Pa·s respectively. The density of this liquid, ρ, is 1015 kg/m^3.

3. Results and Discussion

3.1 Flow velocity in model vessels

We present again the flow velocity of the model vessel with the turbine impeller[3] for comparison with the other types of impeller mixer.

Figure 2 shows the calculated velocity vector distributions in the 6-bladed turbine impeller mixer for $n=3.33\,\mathrm{s}^{-1}$. Figure 2(a) shows that on the r–z plane, discharge flow is dominant at $J=1$, while circulation flows are prominent at $J=4$. The center of both secondary circulation flows can be seen in the vicinity of the impeller blade edge. The flow velocity is very

* The analogy of a Newtonian fluid for 0.2-m to 0.8-m vessels was attained within 6–10% relative error for V_r and 3–7% for V_θ by the authors' analysis.

** We analyze any large-scale vessel with the same numbers of divided cells as a model one. We have confirmed, through the good agreement between the computational and experimental results for the $D=0.4$ m turbine mixer, that the reliability of this method is held up when the flow state is adequately steady.

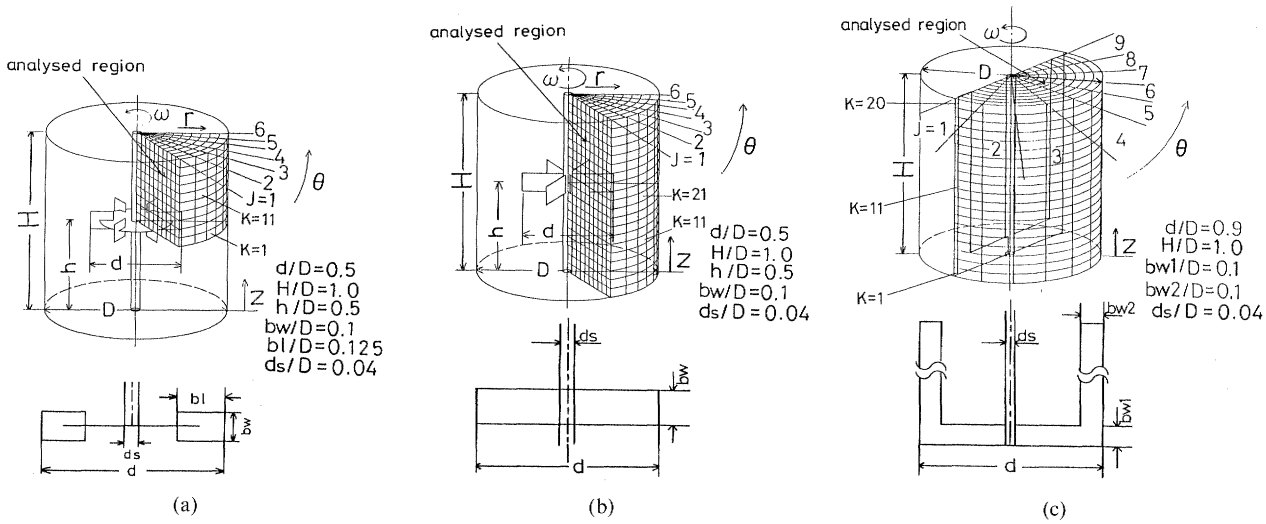

Fig. 1. Scheme of mixers and analysed regions: (a) turbine impeller mixer; (b) paddle impeller mixer; (c) anchor impeller mixer

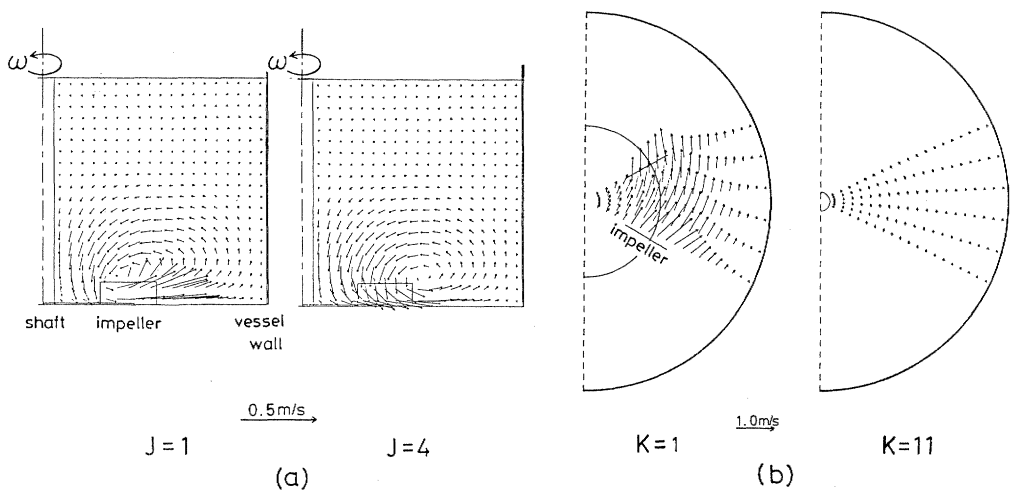

Fig. 2. Velocity vector distributions in turbine mixer ($D=0.2$ m, $n=3.33\,s^{-1}$): (a) on r–z plane at $J=1$ and 4; (b) on r–θ plane at $K=1$ and 11

small at $K=1$ of the inner region of the impeller blade and $K=11$ on the r–θ plane as shown in Fig. 2(b).

Figure 3 shows the velocity vector in the 6-bladed paddle impeller mixer for $n=3.33\,s^{-1}$. From Fig. 3(a), the liquid flow in the upper half of the analyzed region is found to be much the same as that in the lower one. The bottom effect is not so significant. The flow patterns on both r–z and r–θ planes are similar to those in the turbine impeller mixer except for the inner region of the impeller blades, in which notable vertical flows exist because of the absence of a disk plane. **Figure 4** indicates the results in the anchor impeller mixer for $n=0.83\,s^{-1}$. The flows are utterly different from those in the previous mixers. The upward pumping flow generated by the impeller at $J=1$ is strong near the bottom of the vessel. However, the flow velocity decreases rapidly with increasing height of liquid. A weak circulation flow is noticed at $J=5$, and the liquid at $J=9$ is sucked into the back of the impeller. In r–θ plane, the flow develops near the vessel wall in the vicinity of the impellers. The flow at $K=11$ is the same as that at $K=20$ and this implies that two-dimensional flow occurs in the upper region of the vessel.

3.2 Flow analogy in geometrically similar scaled-up vessels

We preliminarily tested the applicability of Eq. (1) for several β values before applying Re_d given by Eq. (4). The mixers are four geometrically similar ones with turbine impeller and having of vessel diameters, $D=0.2$, 0.4, 0.6, and 0.8 m. n_l is set at four values, corresponding to the cases when $\beta=0$, 2/3, 1, and 2, while $d_m=0.1$ m and $n_m=3.33\,s^{-1}$. These rotational speeds are summarized in **Table 1**.

Figure 5 shows the calculated flow velocity components, V_r^* and V_θ^*, normalized by impeller tip velocity, πnd, at $K=1$ in Fig. 1(a). Each flow velocity profile indicates the arithmetic average value in the

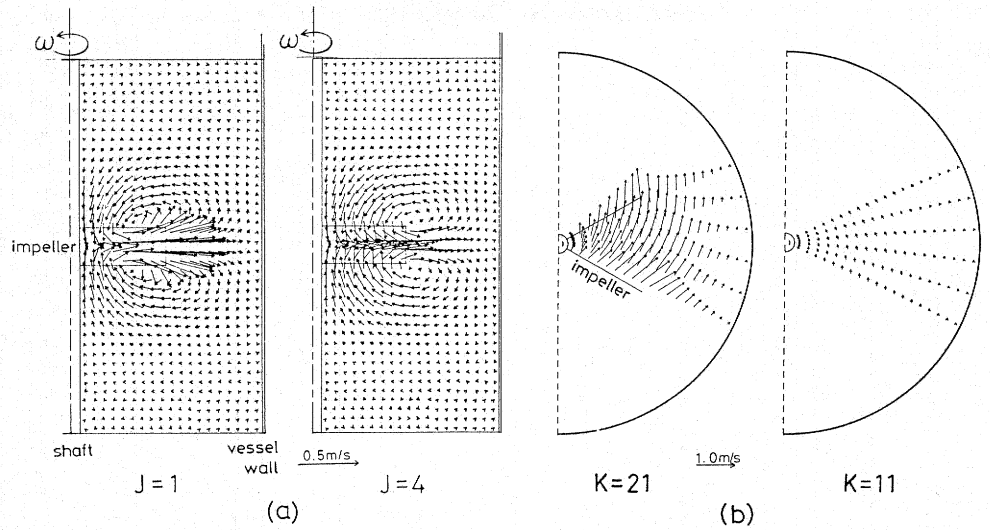

Fig. 3. Velocity vector distributions in paddle mixer ($D=0.2$m, $n=3.33\,s^{-1}$): (a) on r–z plane at $J=1$ and 4; (b) on r–θ plane $K=11$ and 21

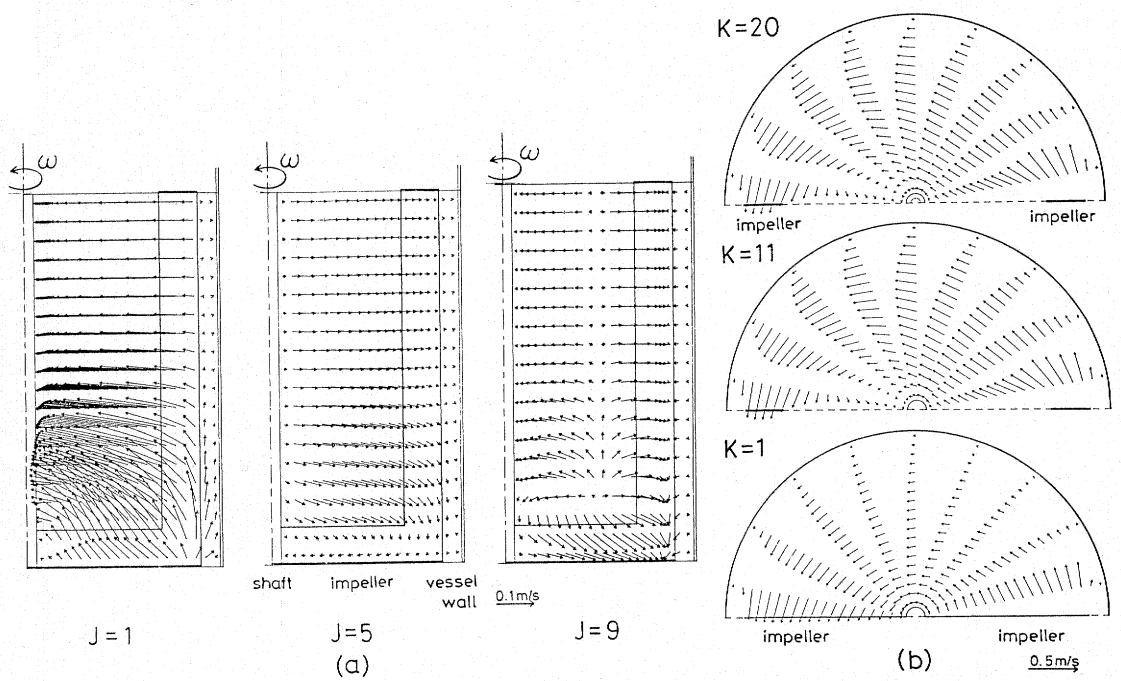

Fig. 4. Velocity vector distributions in anchor mixer ($D=0.2$m, $n=0.83\,s^{-1}$): (a) on r–z plane at $J=1$, 5 and 9; (b) on r–θ plane at $K=1$, 11 and 20

Table 1. Rotational speeds given by Eq. (1) at several β values for 6-bladed turbine mixers

D [m]	d [m]	n [s^{-1}]	β [—]
0.2	0.1	3.33	model
0.4	0.2	0.83	2
0.4	0.2	1.67	1
0.4	0.2	2.10	2/3
0.4	0.2	3.33	0
0.6	0.3	0.37	2
0.6	0.3	1.11	1
0.8	0.4	0.21	2
0.8	0.4	0.83	1

circumferential direction from $J=1$ to 6 for easy comparison between the model and the large vessel. In this figure, the normalized flow velocity profile in the 0.4-m vessel is not consistent with that in the model vessel even if $\beta=2$ as well as other values. The deviation of each profile in the 0.6-m vessel is more remarkable than the previous cases. The disagreement between the profiles in the two scaled-up vessels is due to ignoring the influence of non-Newtonian viscosity distribution in a mixer. The V_θ^* profile at $\beta=2$ in the 0.8-m vessel is closer to that of the model vessel than in the previous case, since n_t is smaller so that the viscosity distribution is less significant. The larger the

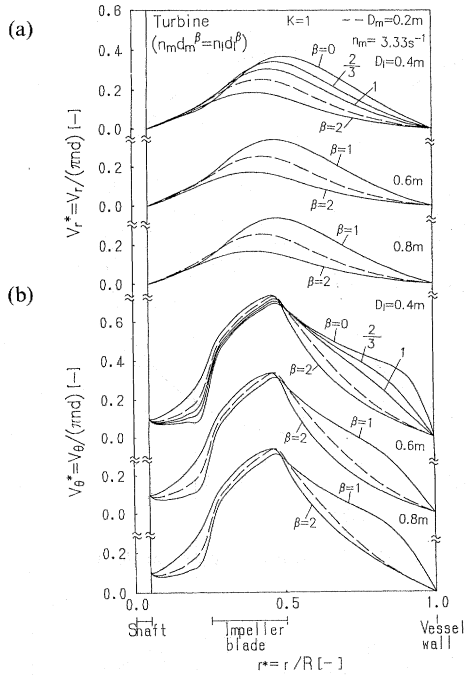

Fig. 5. Profiles of normalized velocities in turbine mixers at several β values for $D=0.2$ to 0.8 m at $K=1$: (a) V_r^*; (b) V_θ^*

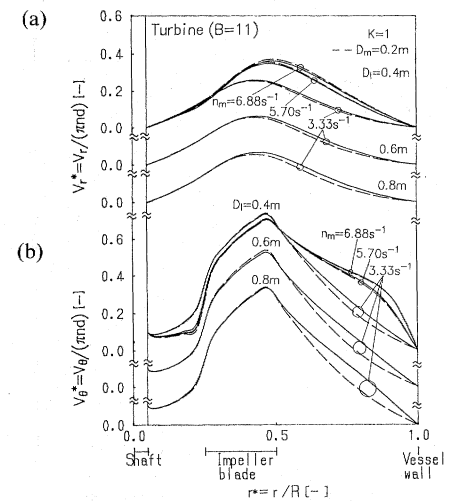

Fig. 6. Profiles of normalized velocities in turbine mixers at $B=11$ for $D=0.2$ to 0.8 m at $K=1$: (a) V_r^*; (b) V_θ^*

value of D_l, the more applicable $\beta=2$ in Eq. (1) to the flow analogy of the pseudoplastic liquid is considered to be.

We then considered the impeller Reynolds number so as to fit the flow velocity distribution of the large-scale vessel to that of the model vessel, as follows. **Figure 6** indicates the velocity profile at $K=1$ in Fig. 1(a) in $D_l=0.4$-m to 0.8-m turbine impeller vessels for n_l calculated by Eqs. (6)-(8). n_l for $D_l=0.4$ m was set at three values corresponding respectively to $n_m=3.33\,s^{-1}$, $5.70\,s^{-1}$, and $6.88\,s^{-1}$. For $D_l=0.6$ m and 0.8 m, n_l was set at the value corresponding to $n_m=3.33\,s^{-1}$. These values of n_m and n_l are tabulated in **Table 2**. The B value used is 11, proposed by

Table 2. Rotational speeds and impeller Reynolds numbers given by Eq. (4) for turbine, paddle and anchor mixers

Impeller type	D [m]	d [m]	n [s^{-1}]	$Re_a=\frac{\rho nd^2}{\eta}$ [—]	B [—]	$\eta\|_{\dot{\gamma}=Bn}$ [Pa·s]
6-bladed turbine	0.2	0.1	3.33	43.8	11*	0.77
	0.4	0.2	1.30	43.8	11	1.20
	0.6	0.3	0.71	43.8	11	1.48
	0.8	0.4	0.44	43.8	11	1.65
	0.2	0.1	5.70	100.2	11*	0.58
	0.4	0.2	2.30	100.2	11	0.93
	0.2	0.1	6.88	134.7	11*	0.52
	0.4	0.2	2.80	134.7	11	0.84
6-bladed paddle	0.2	0.1	3.33	47.9	13*	0.71
	0.4	0.2	1.31	47.9	13	1.12
	0.6	0.3	0.73	47.9	13	1.39
	0.8	0.4	0.46	47.9	13	1.58
Anchor	0.2	0.18	0.83	26.9	25**	1.02
	0.4	0.36	0.30	26.9	25	1.49
	0.6	0.54	0.16	26.9	25	1.71
	0.8	0.72	0.09	26.9	25	1.80

* Proposed by Metzner *et al.*[7,8]
** Proposed by Nagata.[9]

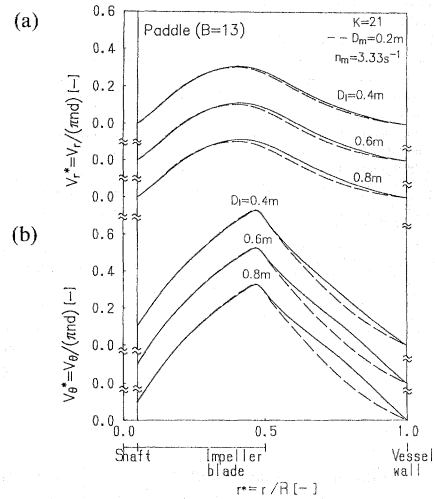

Fig. 7. Profiles of normalized velocities at $B=13$ in paddle mixers for $D=0.2$ to 0.8 m at $K=21$: (a) V_r^*; (b) V_θ^*

Metzner *et al.*[7,8] The normalized flow profiles in the large-scale vessels are in fairly good agreement with that in the model one, in particular within the impeller blade region in which power consumption is most dominant. The higher the value of n_m, the better is the flow similarity attained, while the larger the value of D_l, the larger is the deviation in the flow profile of V_θ^* in the outer region of the impeller blade. **Figure 7** shows V_r^* and V_θ^* profiles calculated by using $B=13$ proposed by Metzner *et al.*[7,8] for the paddle mixers of $D=0.2$ to 0.8 m at $K=21$ in Fig. 1(b) for

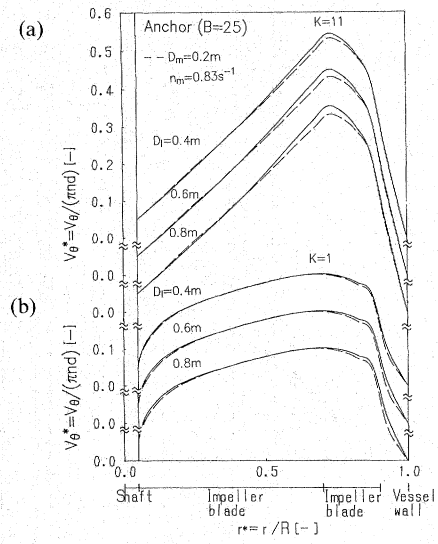

Fig. 8. Profiles of normalized velocities, V_θ^* at $B=25$ in anchor mixers for $D=0.2$ to 0.8 m: (a) at $K=11$; (b) at $K=1$

$n_m=3.33\,s^{-1}$. This figure shows that the normalized velocity profiles except for the inner region of the impeller and the agreement between the two profiles are similar to those of the turbine mixers. The V_θ^* profiles for the anchor impeller mixers of $D=0.2$ to 0.8 m at $K=1$ and 11 in Fig. 1(c) for $n_m=0.83\,s^{-1}$ are shown in **Fig. 8**. n_l is determined by setting B to 25, proposed by Nagata.[9] The profile in the model and those in the large-scaled vessels are in fairly good agreement.

Figure 9 shows the profiles of shear rate normalized by Bn, Γ^*, (a) and of apparent viscosity normalized by η calculated as $\Gamma=Bn$, η^*, (b) for the turbine mixers at $K=1$, calculated by using $B=11$ for $n_m=6.88\,s^{-1}$ and $3.33\,s^{-1}$. The shear rate distribution varies complicatedly in the both radial and circumferential directions and has intrinsic profiles for n_m. The Γ^* profiles for $D=0.4$ m are in agreement with the both model ones regardless of their complexity. $\Gamma=Bn$ is proved to be applicable to the flow analogy of the pseudoplastic liquid. However, the larger the value of D_l, the higher Γ_l^* becomes near the vessel wall compared with Γ_m^*. The η^* profiles of the 0.2-m and 0.4-m vessels are also found to be in fair agreement, while the larger the value of D_l, the lower η_l^* becomes, paticularly near the vessel wall. The deviation of the flow profiles in this region in Fig. 9 is considered to be attributable to the nonlinearity of the Ellis liquid having zero shear viscosity, η_0, while the B value used is determined by the power-law model without using η_0. The Γ^* and η^* profiles calculated by using $B=13$ for the paddle mixers are similar to those of the turbine mixers because of the similarity of the velocity fields. The state of agreement of the shear rate and viscosity profiles is also similar to the previous case. **Figure 10** shows the Γ^* and η^* profiles at $K=11$ under $B=25$

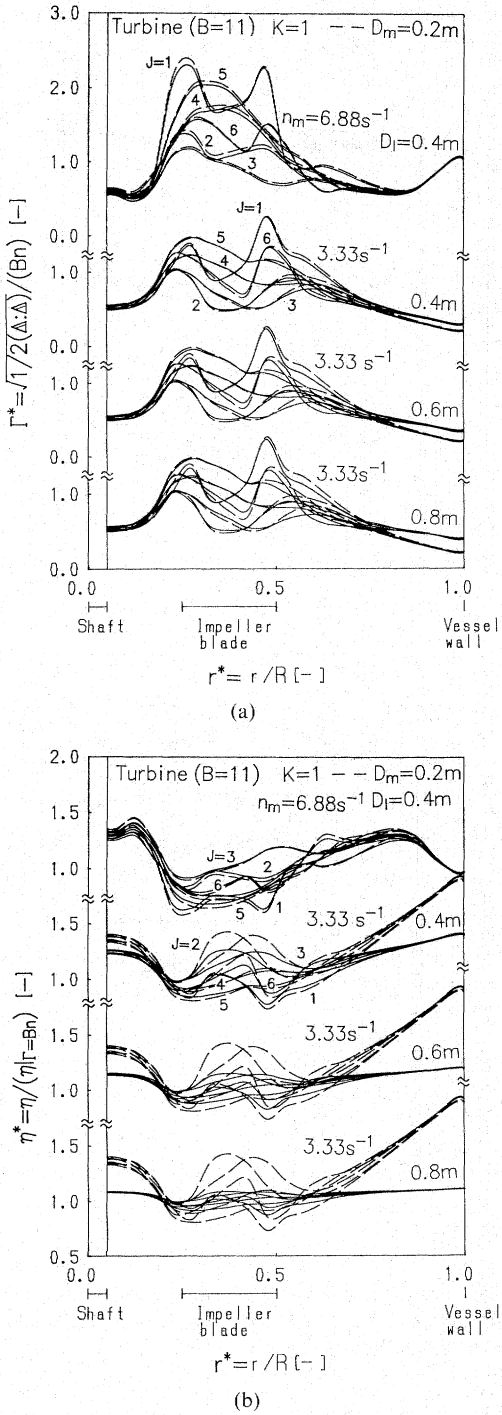

Fig. 9. Profiles of flow behaviour in turbine mixers at $B=11$ for $D=0.2$ to 0.8 m at $K=1$: (a) normalized shear rate; (b) normalized apparent viscosity

for the anchor mixers. Both profiles are fairly flat except around the impeller blade. The agreement of Γ^* between the two scaled-up vessels is very good, while η^* profiles are likely different from each other. The reason why the two η^* profiles are unlikely to fit whilst the two V_θ^* profiles come in fit quite well as shown in Fig. 8 is considered to be that the influence of viscosity becomes insignificant because of the low speed of n_m. **Figure 11** shows the relation between the

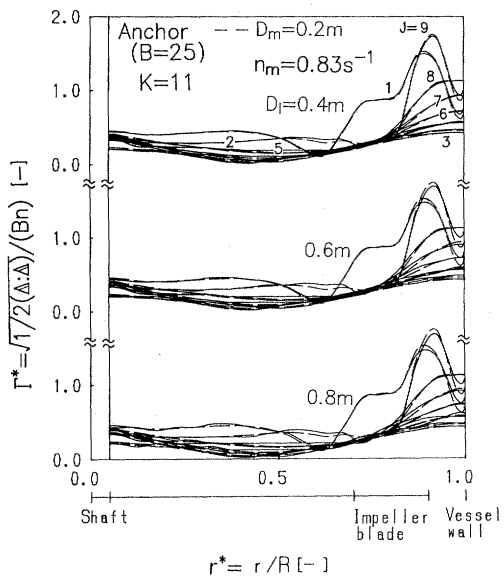

(a)

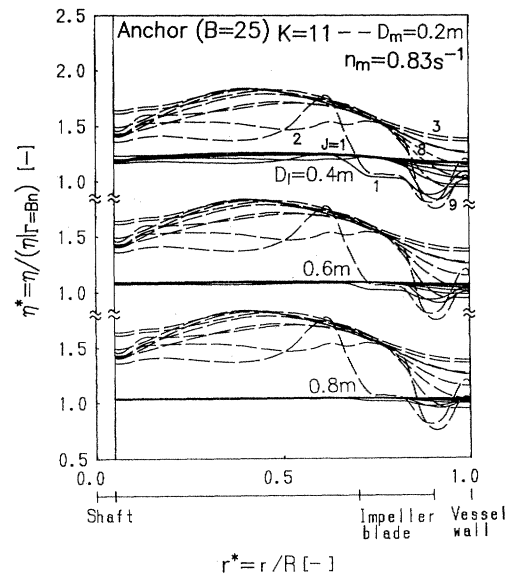

(b)

Fig. 10. Profiles of flow behaviour in anchor mixers at $B=25$ for $D=0.2$ to 0.8 m at $K=11$: (a) normalized shear rate; (b) normalized apparent viscosity

relative errors of flow analogy, ε, in r–θ plane based on the model profile defined by Eq. (9) and scale-up ratio, D_l/D_m.

$$\varepsilon=\frac{1}{N_I N_J}\sum_{I,J}\left|\frac{\Psi_l-\Psi_m}{\Psi_m}\right|_{I,J}\times 100 \qquad (9)$$

Where Ψ represents the normalized variables concerning flow analogy such as V_r^*, V_θ^*, Γ^* and η^*, and N_I, N_J indicate the total discretized mesh numbers in each direction. From this figure, it is found that the flow analogy is attained generally within 20% relative error and that the tendency in discrepancy of analogy is very similar for turbine and paddle mixers.

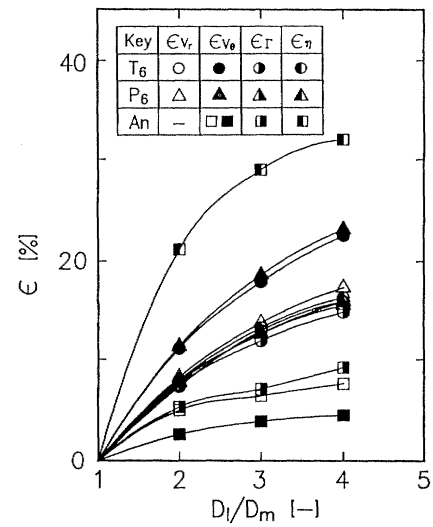

Fig. 11. Relation between relative errors with respect to flow analogy and scale-up ratio (T_6: 6-blade turbine; P_6: 6-blade paddle; An: anchor)

The flow analogy for anchor mixers is almost independent of the analogy in viscosity distribution.

The impeller Reynolds numbers calculated from $\Gamma=Bn$ for all the calculations throughout Figs. 6–10 are tabulated in Table 2. Impeller Reynolds number using $\Gamma=Bn$ is useful for approximately attaining the flow analogy of the Ellis fluid, which gives the basis of power correlation of power-law fluid to Newtonian liquid as proposed by Metzner *et al.*[7,8]

Conclusion

The analogy law regarding the flow of the pseudoplastic Ellis liquid in geometrically similar vessels ranging from 0.2 to 0.8 m vessel diameters with turbine, paddle, and anchor types of stirring impeller was investigated numerically on the basis of the values of B proposed by Metzner *et al.* and Nagata. It was found that the flow analogy in two differently sized vessels was nearly attained in the vicinity of the impeller blade by fitting the impeller Reynolds number using the apparent viscosity calculated by taking the representative shear rate as Bn, where B was set at different values depending on the type of stirring impeller proposed by Metzner *et al.* and Nagata. It was also shown quantitatively that the deviation between the velocity profile in the model and that in the large-scale vessel increased with increasing scale-up ratio in the lower shear rate region.

Acknowledgment

The authors are grateful to Mr. T. Kawakami, of Canon Corporation, and Mr. M. Tsuruta for contributing to a part of the present work. The numerical calculations were carried out by use of the HITAC M-680H and S-820/80 of the Computer Center of University of Tokyo.

Nomenclature

B	=	constant value in Eq. (3)	[—]
b_l	=	length of blade	[m]
b_w	=	width of blade	[m]
D	=	vessel diameter	[m]
d	=	impeller diameter	[m]
d_s	=	shaft diameter	[m]
H	=	height of liquid	[m]
h	=	height of impeller	[m]
I	=	mesh number in r direction	[—]
J	=	mesh number in θ direction	[—]
K	=	mesh number in z direction	[—]
N_I	=	total mesh number in r direction	[—]
M_J	=	total mesh number in θ direction	[—]
n	=	rotational speed of impeller	[s^{-1}]
R	=	radius of vessel ($=D/2$)	[m]
Re_d	=	impeller Reynolds number ($=\rho n d^2/\eta$)	[—]
r	=	radius	[m]
V	=	flow velocity	[m/s]
V^*	=	normalized flow velocity ($=V/(\pi n d)$)	[—]
z	=	height	[m]
α	=	index in Ellis model equation	[—]
β	=	index of scale-up criterion	[—]
Γ	=	representative shear rate in a mixer	[s^{-1}]
Δ	=	rate of deformation tensor	[s^{-1}]
ε	=	relative errors of flow analogy defined by Eq. (9)	[—]
η	=	apparent viscosity	[Pa·s]
η_0	=	viscosity at zero shear rate	[Pa·s]
θ	=	angle	[rad]
μ	=	Newtonian viscosity	[Pa·s]
ρ	=	density	[kg/m^3]
$\tau_{1/2}$	=	half of shear stress	[Pa]
Ψ	=	normalized variable concerning flow analogy	[—]

〈Subscripts〉

l	=	large-scale vessel
m	=	model vessel
r, θ, z	=	axes of cylindrical coordinates

Literature Cited

1) Bertrand, J. and J. P. Couderc: *Chem. Eng. Res. Des.*, **63**, 259 (1985).
2) Hiraoka, S., I. Yamada and K. Mizoguchi: *J. Chem. Eng. Japan*, **12**, 56 (1979).
3) Kaminoyama, M., F. Saito and M. Kamiwano: *Kagaku Kogaku Ronbunshu*, **14**, 786 (1988).
4) Kamiwano, M., R. Saito and N. Ohshima: *Kagaku Kogaku Ronbunshu*, **4**, 588 (1978).
5) Kamiwano, M., N. Ohshima, T. Motoyoshi and F. Shirasaka: *Kagaku Kogaku Ronbunshu*, **5**, 318 (1979).
6) Kamiwano, M., F. Saito and M. Kaminoyama: *Kagaku Kogaku Ronbunshu*, **14**, 316 (1988).
7) Metzner, A. B. and R. E. Otto: *AIChE J.*, **3**, 3 (1957).
8) Metzner, A. B., R. H. Feehs, H. L. Ramos, R. E. Otto and J. D. Tuthill: *AIChE J.*, **7**, 3 (1961).
9) Nagata, S.: "Mixing," p. 78, Kodansha Ltd. Tokyo, Japan (1975).
10) Tomita, Y.: "Rheology," 2nd ed., p. 254, Corona Publishing Co., Ltd. Tokyo, Japan (1975).